

MET.O.14

METEOROLOGICAL OFFICE
BOUNDARY LAYER RESEARCH BRANCH
TURBULENCE & DIFFUSION NOTE



T.D.N. No. 104

FLOW OVER AN ISOLATED HILL OF MODERATE SLOPE

by

P.J.Mason & R.I.Sykes

May 1978

Please note: Permission to quote from this unpublished note should be obtained from the Head of Met.O.14, Bracknell, Berks, U.K.

FH1B

MASTER

Flow over an isolated hill of moderate slope

by P J Mason and R I Sykes

Meteorological Office

Bracknell

Abstract

The two-dimensional theory of Jackson and Hunt (1975) for turbulent flow over a shallow ridge is extended to three-dimensional topography. The results are compared with both the theoretical results for a ridge and with surface wind observations from a nearly circular isolated hill. The agreement between theory and observations is encouraging.

1. Introduction

An understanding of atmospheric flow over topography has many applications including forecasting wind loading on buildings, forest damage, and local pollution transport. If accurate predictions are to be made of wind speeds near the surface, then the fact that the atmospheric flow is turbulent must be taken into account. Taylor (1977) and Deaves (1976) both present numerical models of turbulent boundary layer flow over a two-dimensional ridge, using a mixing length hypothesis to represent the turbulence. It is known that the concept of a mixing length is inadequate for strong perturbations, so the numerical results are expected to be inaccurate for steep topography. This is compounded by our incomplete understanding of non-linear topographic effects (Mason and Sykes 1978, Sykes 1978) and the results of studies employing empirical turbulence models can be difficult to correctly interpret without comparisons with real data. Unfortunately, the data available to compare with model predictions is very limited. Atmospheric observations are mostly restricted to small scale embankments, and extrapolating wind tunnel measurements to atmospheric scales is an uncertain technique.

For gentle topography a preferable approach is the rational theory for flow over a ridge developed by Jackson and Hunt (1975). This theory is based on the known dynamics of the corresponding laminar flow, and uses an eddy viscosity to close the equations; for small perturbations this can be justified using equilibrium boundary layer arguments. At present this is the best starting point for a comparison with atmospheric flow over hills.

In this paper, we present some measurements of the surface flow over a hill, and compare these with the predictions of linear theory. Apart from their immediate interest the observations were made to help quantify requirements for future more detailed studies. The hill chosen for the measurements was Brent Knoll in Somerset. This roughly circular hill with base width 1.3 km and

height 130 m stands isolated on a very flat plain.

The wind speed 2 m above the top of Brent Knoll is roughly double the upstream value, therefore the requirements of a linear theory are not strictly satisfied. However, the comparison is worthwhile as it is not a priori obvious how large the errors in a linear theory will be. To make the comparison, the two-dimensional theory of Jackson and Hunt (1975) has been extended to include three-dimensional effects. The theory is of interest in its own right, since it provides information regarding the differences between two- and three-dimensional flows. In the next section the extension of the theory is presented, and in § 3 some linear results are discussed. § 4 describes the method of data acquisition and analysis whilst the results and comparison with theory are given in § 5.

2. Extension of Jackson-Hunt theory to three-dimensions

If we consider a parallel boundary layer flow approaching the hill, i.e. $u = (u_0(z), 0, 0)$ upstream (see Figure 1), then the extension of the theory to a three-dimensional flow is very simple. This is due to the fact that the theory is linear, hence the induced velocities in the transverse direction do not interact with the streamwise component of velocity.

Formally then, we postulate the same basic structure as Jackson and Hunt. The velocity profile upstream is logarithmic near the surface,

$$u_0(z) = \frac{u_*}{\kappa} \ln \frac{z}{z_0}, \quad z < \delta$$

where u_* is the friction velocity, z_0 the roughness length, and κ is von Karman's constant. δ is the boundary layer thickness, and we assume

$$\begin{aligned} u_0(z) &= \frac{u_*}{\kappa} \ln \frac{\delta}{z_0}, \quad z > \delta \\ &= u_0, \quad \text{say} \end{aligned}$$

This is obviously a crude model of the outer part of the boundary layer. However, Jackson and Hunt (hereafter referred to as JH) show that the results are independent of the precise nature of the match with the free-stream. This is

because the shear at the top of the boundary layer is very small, thus the velocity is essentially constant.

Consider a hill of length scale L in both horizontal directions, and profile $z = hf(x/L, y/L)$ where x and y are the streamwise and cross-stream horizontal co-ordinates respectively, and f is a smooth function with magnitude $O(1)$. We postulate an inner flow region near the surface of thickness ℓ , where ℓ is determined by a balance of terms in the equations of motion. Define non-dimensional co-ordinates $X = x/L$, $Y = y/L$, $Z = (z - hf(x, y))/\ell$, so that Z is the dimensionless distance above the surface. The analysis is identical to that in \mathcal{JH} , therefore the details are omitted here. \mathcal{JH} assume that the solution for the streamwise component of velocity consists of the upstream velocity profile displaced vertically by an amount $hf(x, y)$, plus a small perturbation, viz

$$u(x, y, z) = u_0(z - hf(x, y)) + \varepsilon u_* U(X, Y, Z) \quad (2.1)$$

where ε is to be determined.

ε and ℓ are chosen to give a balance between inertial, pressure, and diffusion terms in the inner layer, the pressure being generated in the outer layer by the vertical displacement. Since the pressure gradient in the y -direction is of the same order as that in the x -direction, a transverse velocity of order εu_* will also be induced.

$$\text{ie. } v(x, y, z) = \varepsilon u_* V(X, Y, Z)$$

It is shown in \mathcal{JH} that the equation for U is

$$\frac{\partial U}{\partial X} = - \frac{\partial P}{\partial X} + \frac{\partial}{\partial Z} \left(Z \frac{\partial U}{\partial Z} \right) \quad (2.2)$$

where $P(x, y)$ is the pressure field generated by the external flow. Note that since the equations are linearised, the transverse velocity V does not appear in the U -equation. Furthermore, the V -equation is easily obtained analogously as

$$\frac{\partial V}{\partial X} = - \frac{\partial P}{\partial Y} + \frac{1}{2} \frac{\partial}{\partial Z} \left(Z \frac{\partial V}{\partial Z} \right) \quad (2.3)$$

The factor of 2 in the diffusion term is due to the fact that there is no mean flow in the y-direction.

JH show that $\frac{L}{l} \ln \frac{l}{z_0} = 2\kappa^2$, and $\varepsilon = \frac{h}{L} \frac{\ln^2(L/z_0)}{\kappa \ln(l/z_0)}$. They also show that the pressure perturbation has magnitude $\varepsilon \rho u_*^2 \ln(l/z_0)$ where ρ is the density. This defines the magnitude of the pressure in both inner and outer layers, since they must match. The outer layer has a vertical scale of $O(L)$, so we define $z = z/L$. Then $p = \varepsilon \rho u_*^2 \ln(l/z_0) p_1(x, y, z)$ is the first term in the expansion of the outer pressure. The outer flow is inviscid and irrotational, so

$$\nabla^2 p_1 = 0 \quad (2.4)$$

where
$$\nabla^2 = \frac{\partial^2}{\partial x^2} + \frac{\partial^2}{\partial y^2} + \frac{\partial^2}{\partial z^2}.$$

The lower boundary condition for (2.4) is obtained by matching with the vertical velocity at the top of the inner layer. Now the leading term in the vertical velocity is due to the displacement of the upstream profile, as shown in JH. Thus the outer flow is simply inviscid, irrotational flow over the surface $z = f(x, y)$, and the pressure field is determined only by the shape of the topography, with the boundary condition on (2.4) given by

$$\frac{\partial p_1}{\partial z} = - \frac{\partial^2 f}{\partial x^2} \quad \text{on } z = 0. \quad (2.5)$$

The above result comes from the dimensionless vertical momentum equation,

$$\frac{\partial w}{\partial x} = - \frac{\partial p_1}{\partial z}$$

together with the fact that the dimensionless vertical velocity $w = \frac{\partial f}{\partial x}$.

Scalings for these quantities are given in JH.

The above equations are solved by means of the Fourier transform. Define

$$\tilde{u}(k, m, z) = \iint u(x, y, z) e^{-i(kx + my)} dx dy$$

Then
$$\tilde{p} = \tilde{p}_1(k, m, 0) = - \frac{k^2}{(k^2 + m^2)^{1/2}} \tilde{f}$$

and

$$\tilde{u} = \frac{k^2}{(k^2 + m^2)^{1/2}} \left[1 - \frac{K_0(2(ikZ)^{1/2})}{K_0(2(ikZ_0)^{1/2})} \right]$$

$$\tilde{v} = \frac{km}{(k^2 + m^2)^{1/2}} \left[1 - \frac{K_0(2(ikZ)^{1/2})}{K_0(2(ikZ_0)^{1/2})} \right]$$

where $Z_0 = z_0/\ell$, $(ikZ)^{1/2}$ is defined with a branch-cut along the positive imaginary axis with $-\frac{3\pi}{2} < \arg k \leq \frac{\pi}{2}$, and K_0 is the modified Bessel function.

The perturbation stress is obtained exactly as in \mathcal{H} , i.e. the dimensionless perturbation surface stress in the x-direction is

$$\frac{\tilde{\tau}_x - \rho u_*^2}{\epsilon \rho u_*^2} = 2K(ikZ_0)^{1/2} \frac{k^2}{(k^2 + m^2)^{1/2}} \frac{K_1(2(ikZ_0)^{1/2})}{K_0(2(ikZ_0)^{1/2})}$$

and that in the y-direction similarly is

$$\frac{\tilde{\tau}_y}{\epsilon \rho u_*^2} = 2K(2ikZ_0)^{1/2} \frac{km}{(k^2 + m^2)^{1/2}} \frac{K_1(2(2ikZ_0)^{1/2})}{K_0(2(2ikZ_0)^{1/2})}$$

Clearly, the solution for the streamwise component of velocity and surface stress only differs from the corresponding two-dimensional solution as a result of the different driving pressure gradient. The linear solutions for a particular shape and scale of topography are calculated in the next section and the two- and three-dimensional cases are compared.

3. The form of the linear solutions

The shape of the hill used for the three-dimensional results in this section is

$$f(X, Y) = \begin{cases} \cos^2\left(\frac{\pi}{2}(X^2 + Y^2)^{1/2}\right) & , X^2 + Y^2 < 1 \\ 0 & , X^2 + Y^2 \geq 1 \end{cases}$$

The two-dimensional ridge has same cross-section as the centre-line cross-section of the above hill, i.e. $f(X, 0)$. In order to obtain numerical values, $Z_0 = z_0/\ell$ must be specified. We have chosen $Z_0 = 6.9 \times 10^{-4}$ in this case, which corresponds to the Brent Knoll case, where $L = 600$ m, and $z_0 = 2$ cm. These length scales define an inner scale, $\ell = 29$ m.

The Fourier transforms were inverted using a two-dimensional Fast Fourier Transform routine. This precludes the study of isolated topography, since only a finite number of Fourier modes are retained. Thus the real domain is periodic

in both the x- and y-directions. However the domain can be made sufficiently large for the local flow in the vicinity of the hill to be unaffected by the periodicity.

The complex Bessel functions were calculated using the series expansion (Abramowitz and Stegun 1968) which converges rapidly for moderate values of the argument. However, although the series has infinite radius of convergence, large values of the argument give highly inaccurate results due to finite arithmetic. For this reason, the asymptotic form for large argument was used when the modulus of the argument exceeded 5, and the two calculation methods were found to match well.

Figure 2 shows the perturbation velocity fields in the streamwise and cross-stream directions respectively at a dimensionless height $Z = 6.9 \times 10^{-2}$, i.e. $Z = 100 Z_0$. The dashed circle has unit radius and indicates the extent of the topography. The streamwise component shows the expected speed-up over the crest of the hill, with reductions upstream and downstream. The cross-stream component shows the tendency of the fluid to flow around the hill, the fluid moves outward from the centre-line, $Y=0$, upstream of the crest, and is drawn back toward the centre in the lee. These qualitative effects are precisely those expected as a result of the pressure field. However, the quantitative details of the velocity field near the surface are determined by eddy diffusivity.

Centre-line velocity profiles from the above solution are compared with the corresponding results for the two-dimensional ridge in Figure 3. The magnitude of the perturbation velocity is larger in the two-dimensional case. However, the differences are not great, the maximum value in the three-dimensional solution is 1.45 compared to 1.84 in the two-dimensional case. Furthermore, the structure of the profiles is very similar in both cases.

The surface stresses for the two cases are presented in Figure 4. As expected from the velocity profiles, the maximum stress on the ridge is somewhat larger than that on the circular hill. The strong minima upstream and downstream are much more pronounced than those contained in the surface stress results of

Jackson and Hunt. This is a result of the sharper topography used here, and implies that the turbulent boundary layer would separate very easily over this shape of hill. Finally, it can be seen that the three-dimensional flow recovers from the perturbation much more quickly downstream. The periodicity of the domain accounts for the fact that the perturbation stress does not return to zero but the length is sufficient to distinguish upstream and downstream effects. It is also clear that the ridge has greater upstream influence.

4. Data acquisition and analysis

(a) Choice of topography

The present study was intended to be limited in its extent and help quantify requirements for future more detailed work. For this reason an important consideration in choosing the site was reasonable proximity to Bracknell and Porton (the instrumentation and the majority of observers came from the Meteorological Office, Porton). The more scientific factors were

1. a simple smooth shape
2. isolated on a flat plain
3. adequate sites for measurements at 2 m
4. steep enough slopes to give changes which can be easily measured.

The roughly circular hill of Brent Knoll (see Figures 5 and 6) represented the best compromise which we could find. It is fairly smooth in shape and extremely well isolated on a very flat plain. The land use is primarily grazing and affords excellent sites for measurements. The anemometer sites chosen on the flat terrain had good exposure being at least 30 obstacle heights downstream of obstacles such as hedges. Those on the hill were at least 10 obstacle heights downstream. Irregularities in shape were probably the main limitation in accuracy on the hill and the results presented here are from the smooth upper parts and the Eastern side of the hill.

(b) Instrumentation

The majority of measurements were made with Porton anemographs (Jones 1965, 1970) at a height of 2 m perpendicular to the terrain. This height was chosen to keep the measurement system easily portable. Most measurements were only of ten minutes duration, and a team of two people were able to complete measurements at about 10 different sites in four hours. To simplify data processing the anemometer outputs were electrically filtered with a time constant of 10 s. The records from each site were processed to obtain a value for the mean wind speed and direction and the maximum and minimum speeds obtained in the 10 minute record. For the range of wind speeds that we measured (3 to 40 ms^{-1}) the accuracy of the processed data is about $\pm 5\%$ in speed and $\pm 5^\circ$ in direction. In some instances run-of-wind anemometers were used and wind directions were taken from small wind socks; this data had an instrumental accuracy of about $\pm 5\%$ in speed and $\pm 10^\circ$ in direction.

(c) Measurement procedure

The synoptic situations chosen for the experiment were intended to be of fairly neutral vertical stability and free from frontal systems or significant mesoscale disturbances. On suitable days staff travelled to the area and carried out measurements over a four hour period. Continuous records were obtained on about 3 fixed sites and 10 minute observations at an additional 40 sites.

(d) Data analysis

A number of factors had to be considered in the data analysis. About half of the 10 minutes observations were made on the flat terrain surrounding the hill. We anticipated that such measurements about one and two kilometres downstream of the hill would give results regarding the extent of downstream stress reductions. The mean flow speeds 1 km downstream did appear to be systematically about 20% less than those upstream or those 2 km downstream, but this result is barely significant. The difficulty we had with this data arose from mesoscale variations in wind speed occurring with a time scale of one or two hours and having a

peak to peak amplitude in 10 min samples of mean wind of about $\pm 20\%$.

With sites spaced less than about one kilometre apart these variations were similar at both sites but with sites further apart we obtained, even over the same period of time, excellent correlation between some sites, and virtually none between others. The higher correlations always seemed to be roughly along the surface wind directions. This behaviour leads us to suggest that large-scale boundary layer (Ekman) rolls may have been present. The magnitude and nature of the variations we observed was consistent with previous detailed observations of such rolls (Lemone 1973). The meteorological conditions under which the observations were made were all typical of those under which these rolls may be expected i.e. moderate winds and near neutral conditions. We would not have been so disappointed with this result had not single site measurements at Porton, under similar conditions, given a typical scatter of less than $\pm 10\%$. All this data was for westerly type winds and it seems possible, bearing in mind the more frequent observation of regular cloud patterns at sea, that the absence of upstream topography promotes larger amplitude regular boundary layer rolls. Because of these large $\pm 20\%$ variations in wind speed the data over the flat terrain has had to be disregarded, except for providing a value for the undisturbed wind over level terrain. The data from the hill where the observed changes are about $\pm 100\%$ in mean wind speed are not seriously affected.

To help correct for these variations and longer term trends

the data from the hill has been normalised with respect to the mean speed and direction measured on the top of the hill. The upstream speed over flat terrain was taken from the 4 hour means at the other fixed sites. The correction of the data for speed variations is a simple matter involving multiplication by the appropriate ratio \bar{u}/\bar{u}_t where \bar{u}_t is the mean speed on the top of the hill averaged over the time of the observation, and \bar{u} is the overall mean. The correction of changes in wind direction is not so straightforward. This is because as the wind direction changes so the position of the observation point on the hill changes relative to the wind direction. To effect the direction

corrections we have been forced to plot the data on an idealised circular contour map rather than the real map. Each observation site has been assigned a value of radius from the centre of the hill and an angle ψ where ψ is based on the direction of the horizontal tangent at the site rather than the actual angular co-ordinate on the real map. If the overall mean wind direction is $\bar{\theta}$ and $\bar{\theta}_t$ the mean during the period of the observation then the co-ordinate of the observation point (r, ψ) are changed to $(r, \psi - (\bar{\theta}_t - \bar{\theta}))$ and the wind direction γ changes to $\gamma - (\bar{\theta}_t - \bar{\theta})$. The size of the corrections in wind speed and direction were at most $\pm 30\%$ and $\pm 20^\circ$ respectively.

5. Experimental results and comparison with linear theory

The data presented in this section were gathered on a number of separate occasions. Measurements were made spanning a range of upstream wind speeds at 2m from 4 ms^{-1} up to 20 ms^{-1} . In each case, the ratio of speed on the summit to that upstream was essentially the same, confirming the Reynolds number independence of the flow. Thus the results are presented as a composite of the observations on four separate occasions for which the most intensive coverage of the hill was obtained. Figure 7 shows the observed wind speeds at 2 m plotted on an idealised contour map of the topography as described in the previous section. The outer circle represents the base of the hill with a radius of 600 m, and other height contours are indicated at 50 m, 90 m and 130 m. The periods of the four sets of data, together with their mean upstream wind speeds and directions are as follows:

1. 8 November 1977, 1200-1600Z, 4.5 ms^{-1} from 210°
2. 14 November 1977, 1300-1700Z, 14 ms^{-1} from 290°
3. 14 November 1977, 1900-2300Z, 14 ms^{-1} from 300°
4. 15 November 1977, 1100-1600Z, 10 ms^{-1} from 310°

All the data has been scaled to correspond to an upstream wind speed of 10 ms^{-1} , and rotated to give a wind from 270° , as indicated by the large arrow on the left of the diagram. The general consistency of the observations is obvious, and the scatter between adjacent points suggests an error of order $1\text{-}2 \text{ ms}^{-1}$.

The speed-up factor, i.e. the ratio of maximum wind speed to the upstream value is fairly accurately 2.2-2.3, and the minimum wind speed in the lee is about 4 ms^{-1} . The general pattern of the flow is also easily discernible, with air slightly deflected around the hill.

On two occasions, a number of pilot balloon ascents were conducted upstream of the hill during the experiment. These provide an upstream vertical wind profile, and ensure that there are no peculiarities of the incident flow which may produce anomalous data around the hill. Four or five ascents were made throughout each experimental period, and these results were averaged to give a mean profile, which was then scaled to correspond to a 2 m wind of 10 ms^{-1} . The two profiles are presented in Figure 8, which illustrates the general uniformity of the profile. The differences between the two observed profiles are within the expected experimental accuracy. Profiles were not available for every experiment, but the results in Figure 8 suggest that in steady fairly neutral conditions, the incident flow will be near-logarithmic, i.e. below 250 m the boundary layer is in equilibrium. We note that the wind speed over flat ground at the height of Brent Knoll is about 1.75 times the 2 m wind.

Results from the linear theory described in section 2 were obtained using parameters appropriate to Brent Knoll, i.e. $L = 600 \text{ m}$, $h = 130 \text{ m}$, $z_0 = 2 \text{ cm}$. The roughness length was obtained from profiles up to 4 m on the most exposed sites in the area, and is typical of grazing fields. The theory is not very sensitive to z_0 , so although a 4 m profile does not give an accurate roughness length, the errors do not materially affect the results. The hill shape was assumed circular to compare with the results which are plotted on the idealised circular hill. However, the radial profile of the hill was chosen to correspond as closely as possible to the general shape of Brent Knoll, which has a fairly steep slope near the summit. The shape used in the theory is illustrated in Figure 9.

The dimensionless velocity produced by the theory is multiplied by the appropriate scale and added to the basic velocity of 10 ms^{-1} in the x-direction. The resulting wind speeds and directions are illustrated in Figure 10, where the

dashed circle represents the base of the hill, i.e. 600 m radius from the centre. The maximum speed attained on the front edge of the summit is 20.4 ms^{-1} , giving a speed-up factor of 2.0. The minimum in speed in the lee is 6.3 ms^{-1} . The magnitude of the deflections around the hill and speeds around the sides are also similar to those observed. Having regard to the amplitude of the perturbations, agreement between the theory and the observations is quite good. The results depend on the exact shape of the assumed profile, and it must be emphasised that no attempt was made to 'optimise' the theoretical results; the hill profile shown in Figure 9 was chosen solely for its similarity to the shape of Brent Knoll.

Some further results from the experiment are worth describing in a qualitative manner. The Porton anemographs were recording continuously for 10 minutes with a time constant of 10 s (i.e. similar to standard meteorological instruments), so it was possible to extract a maximum and minimum speed over this period. Such a measurement is usually assumed to be related to the magnitude of the turbulent kinetic energy. In fact, we found that the difference between the maximum and the minimum speeds at each site was about 80% of the upstream value and varied by no more than 10% between different sites on each occasion, the variation appearing random. Thus the fluctuations were sufficiently large to reverse the wind direction in the lee of the hill, but were no larger on the summit.

Finally, one experiment was conducted under fairly stable nocturnal conditions. The results showed an enormous speed-up from an upstream wind speed of 1.5 ms^{-1} to about 10 ms^{-1} on the summit of the hill. However this result was obviously due to an extreme velocity profile upstream, with very low wind speeds near the surface, thus the results are not quantitatively useful and are not presented here. However, it was clear from the measurement that the stability of the air was forcing it to flow more around the hill than in the neutral case. The deflections observed were almost 3 times as large as those in Figure 7.

6. Summary

Measurements of wind speed and direction for flow over an isolated hill have been found to form a consistent pattern. In neutral conditions, the pattern does not depend on the wind speed, as expected for such a high Reynolds number flow. The three-dimensional theory of

turbulent flow over a low hill gives reasonable predictions of the observed velocities on Brent Knoll. In particular the speed-up at 2m was observed to be approximately 2.3, while the value predicted by the theory was 2.0.

Acknowledgments

We would like to express our thanks to all the staff who took part in the experiment, for their care in making the measurements and also to the farmers in the Brent Knoll area for their kind cooperation. We would also like to thank in particular Mr A G Sills of Met. Office, Porton Down, for organising the instrumentation and data analysis.

References

- | | | |
|--|------|---|
| Abramowitz, M. and
Stegun, I. (eds) | 1968 | Handbook of mathematical functions, Dover
Publications, New York. |
| Deaves, D.M. | 1976 | 'Wind over hills : a numerical approach'
J Ind Aerodyn. <u>1</u> p 371. |
| Jackson, P.S. and
Hunt, J.C.R. | 1975 | 'Wind flow over a low hill' Q.J.Roy. Met. Soc.
<u>101</u> p 929. |
| Jones, J.I.P. | 1965 | 'A portable sensitive anemometer with proportional
d.c. output and a matching wind velocity-component
resolver'.
J. Sci. Inst. <u>42</u> p 414. |
| | 1970 | 'A new recording wind vane'.
J. Phys. E. <u>3</u> p 9. |
| Mason, P.J. and
Sykes, R.I. | 1978 | 'Separation effects in Ekman layer flow over
ridges' Submitted to Q.J.Roy.Met.Soc. |
| Sykes, R.I. | 1978 | 'Stratification effects in boundary layer flow
over hills'. To appear in Proc.Roy.Soc. |
| Taylor, P.A. | 1977 | 'Numerical studies of neutrally stratified
planetary boundary layer flow above gentle
topography. I two-dimensional case'. Boundary
Layer Met. <u>12</u> p 37. |

Legends

- Figure 1 Schematic geometry of the linear theory.
- Figure 2 Perturbation velocity components for three-dimensional flow at $Z = 6.9 \times 10^{-2}$, with $Z_0 = 6.9 \times 10^{-4}$. (a) streamwise component, u ; (b) transverse component, V . Solid contours represent positive values, dashed contours negative values. The contour interval in (a) is 0.2, and 0.1 in (b).
- Figure 3 Vertical perturbation velocity profiles from two- and three-dimensional solutions.
- Figure 4 Dimensionless surface stress, $\hat{\tau} = (\tau_x - \rho u_*^2) / \epsilon \rho u_*^2$.
- three-dimensional case
----- two-dimensional case
- Figure 5 Schematic map of Brent Knoll area.
- Figure 6 Contour map of Brent Knoll.
- Figure 7 2 m wind observations on and around Brent Knoll. Wind speeds are indicated on the arrows.
- Figure 8 Upstream velocity profiles, two cases denoted by open circles and crosses.
- Figure 9 Idealised profile of Brent Knoll
- Figure 10 Linear theory predictions of 2 m wind
- (a) wind speed, contour interval 2 ms^{-1} .
(b) wind directions.

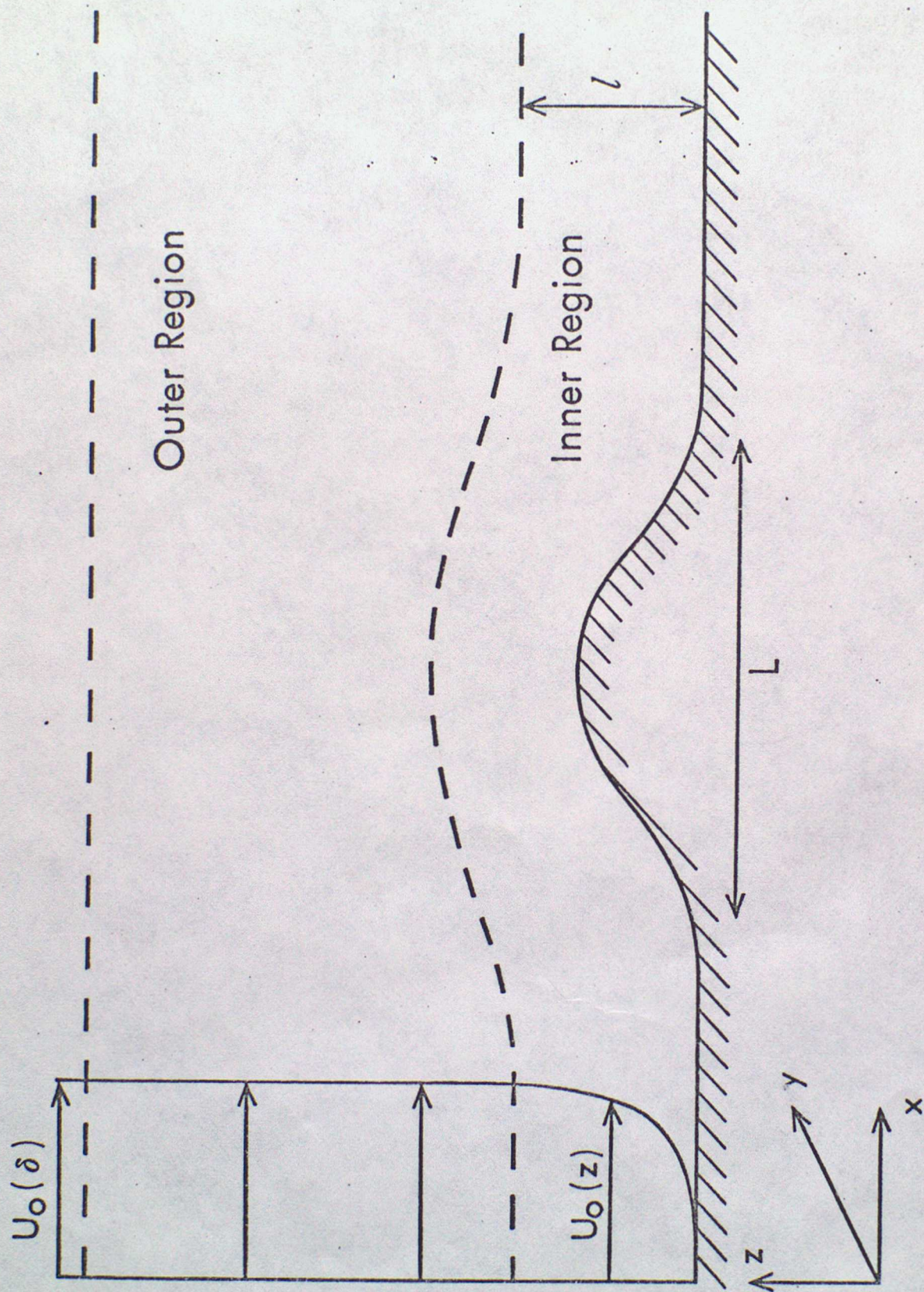
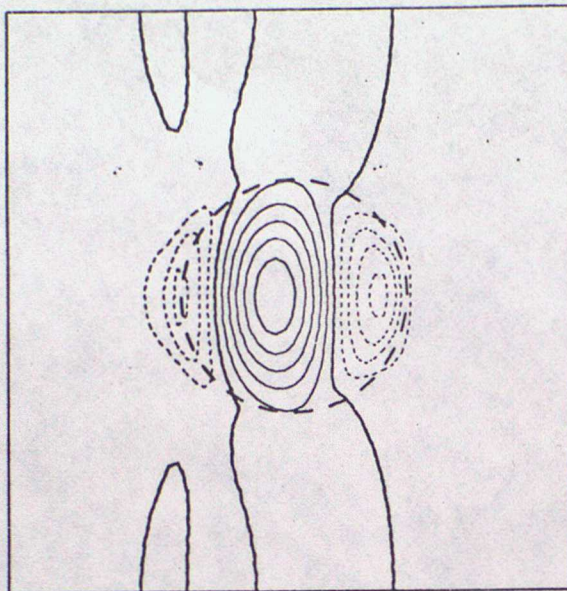


Fig. 1

U-FIELD



V-FIELD

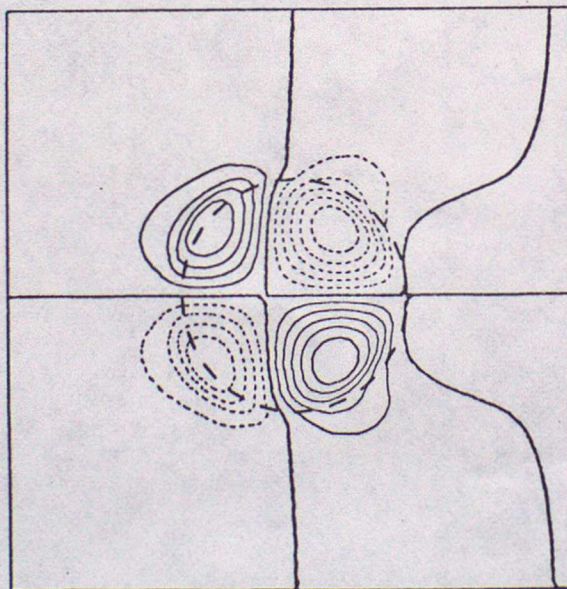


Fig. 2

Ridge

1.0

Circular
hill

1.0

Fig 3

2.0

1.0

X

0

-1.0

-2.0

Z

0.5

0

Z

0.5

0

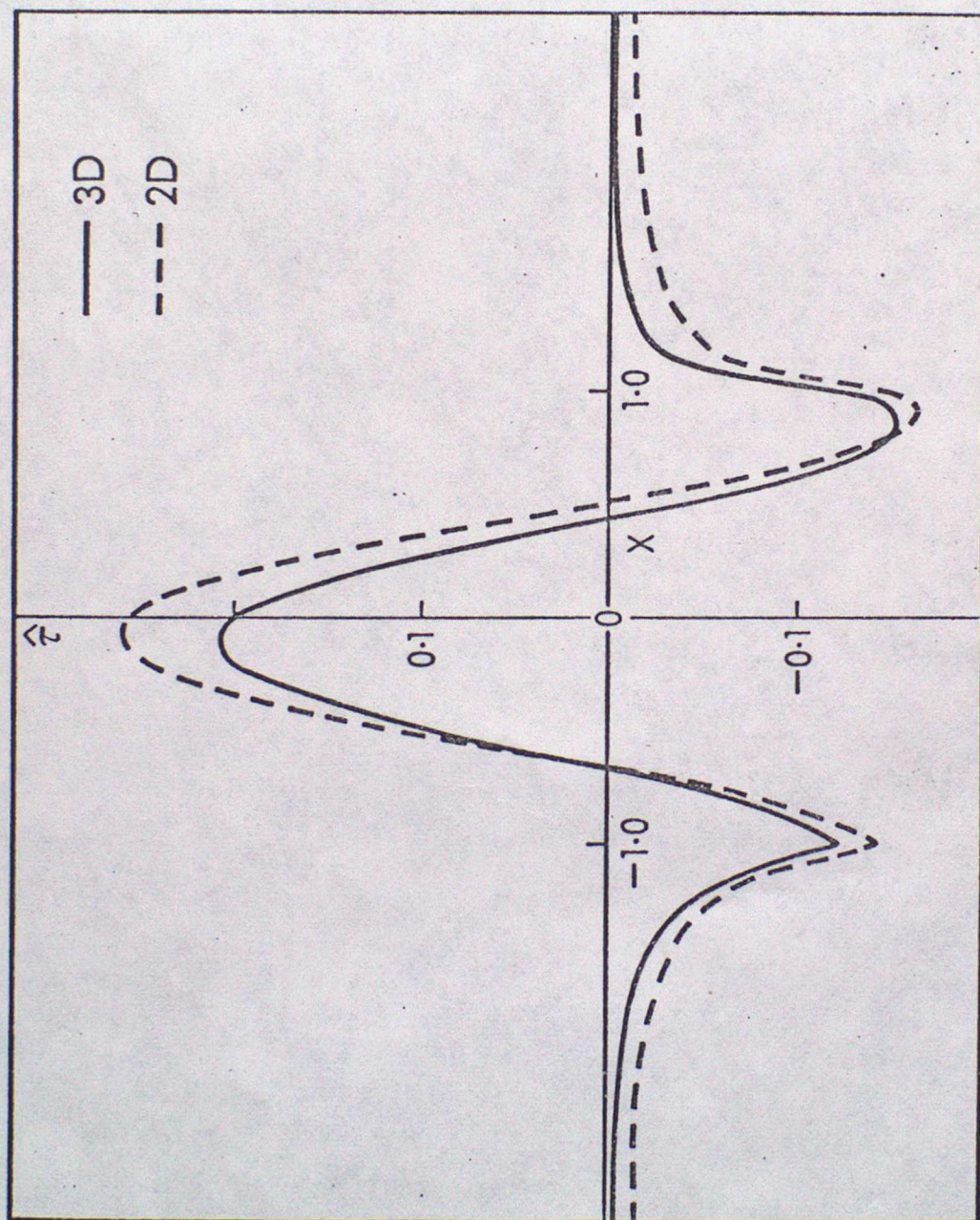


Fig 4

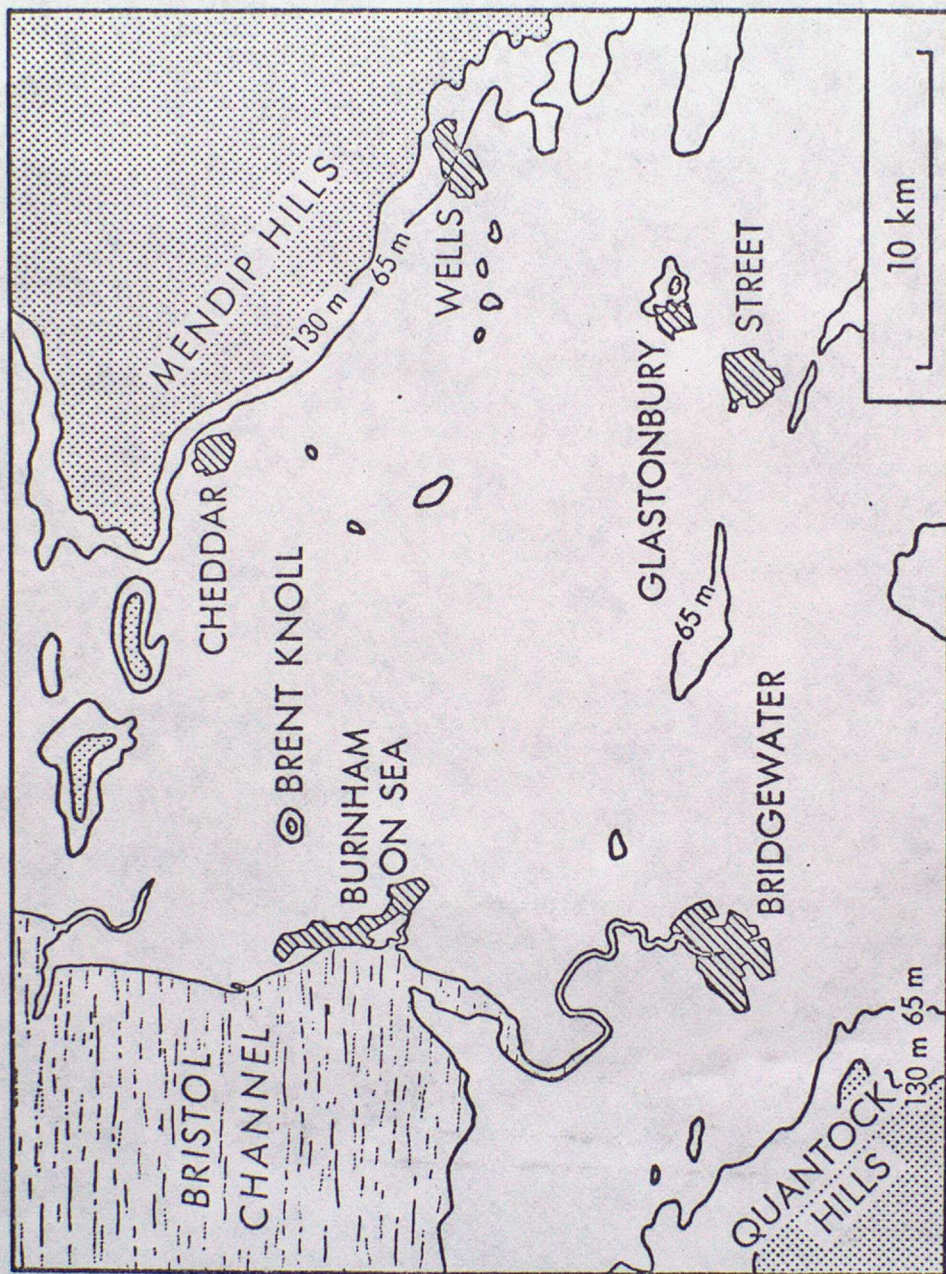


Fig 5

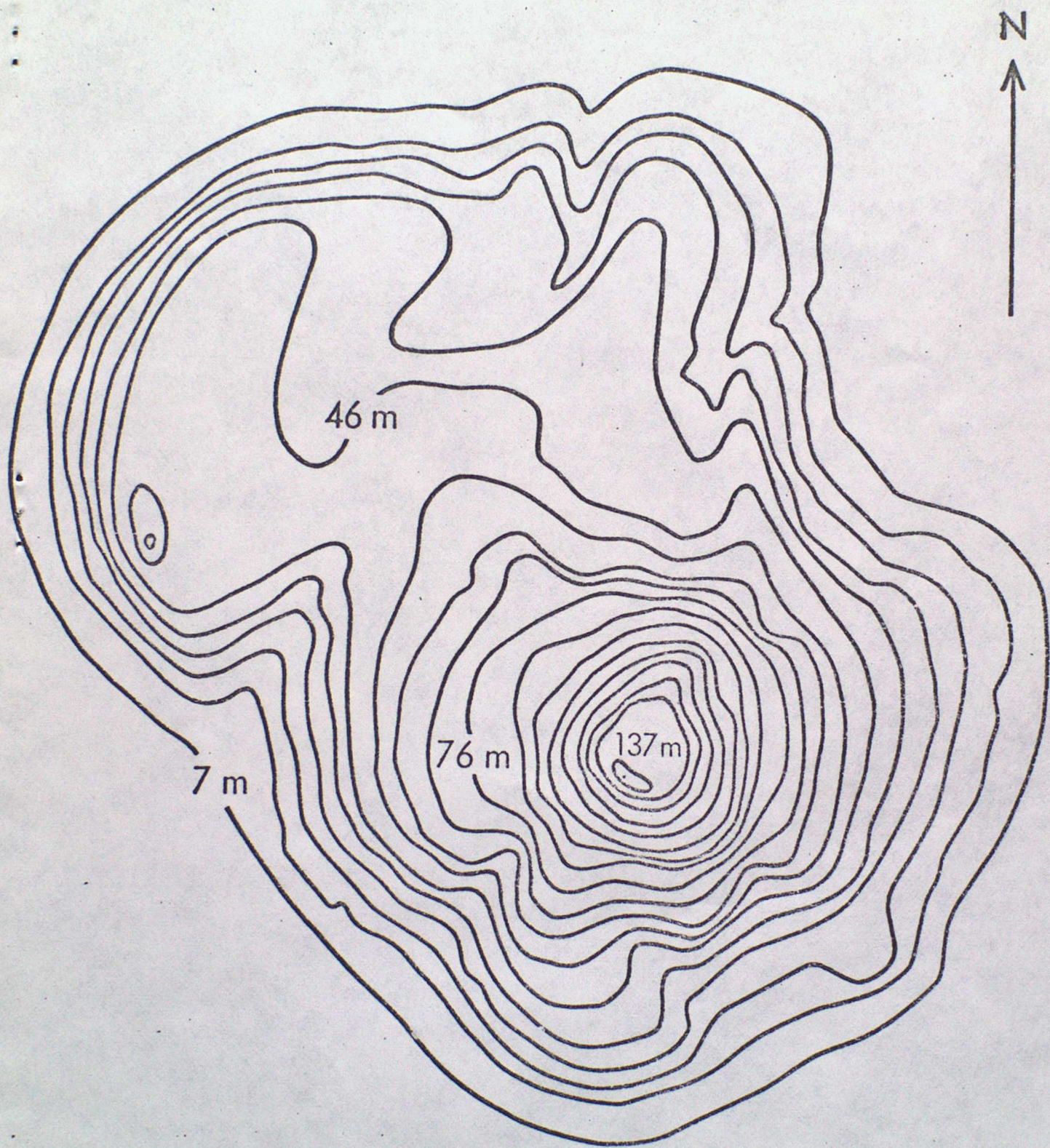
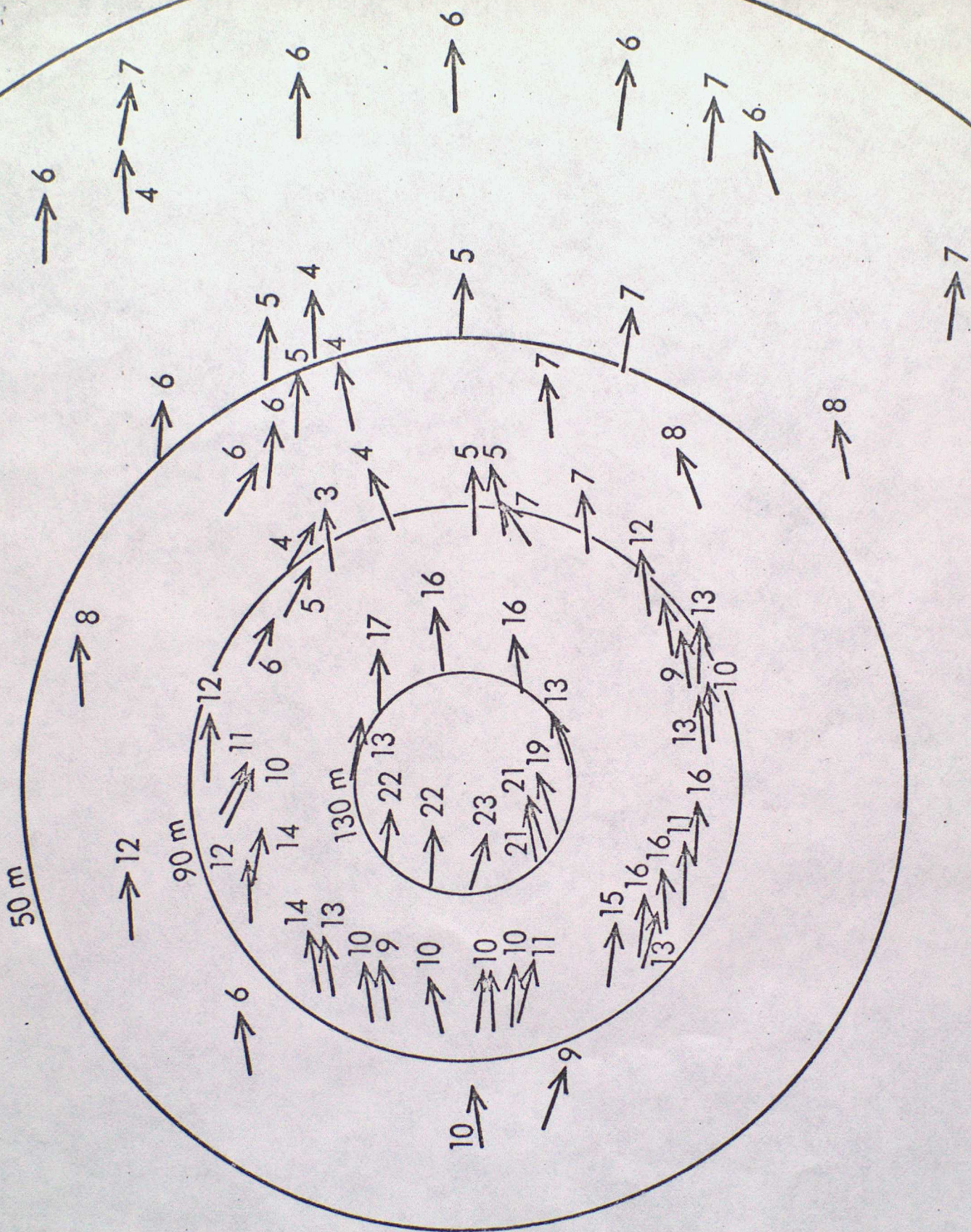


Fig 6



7

10

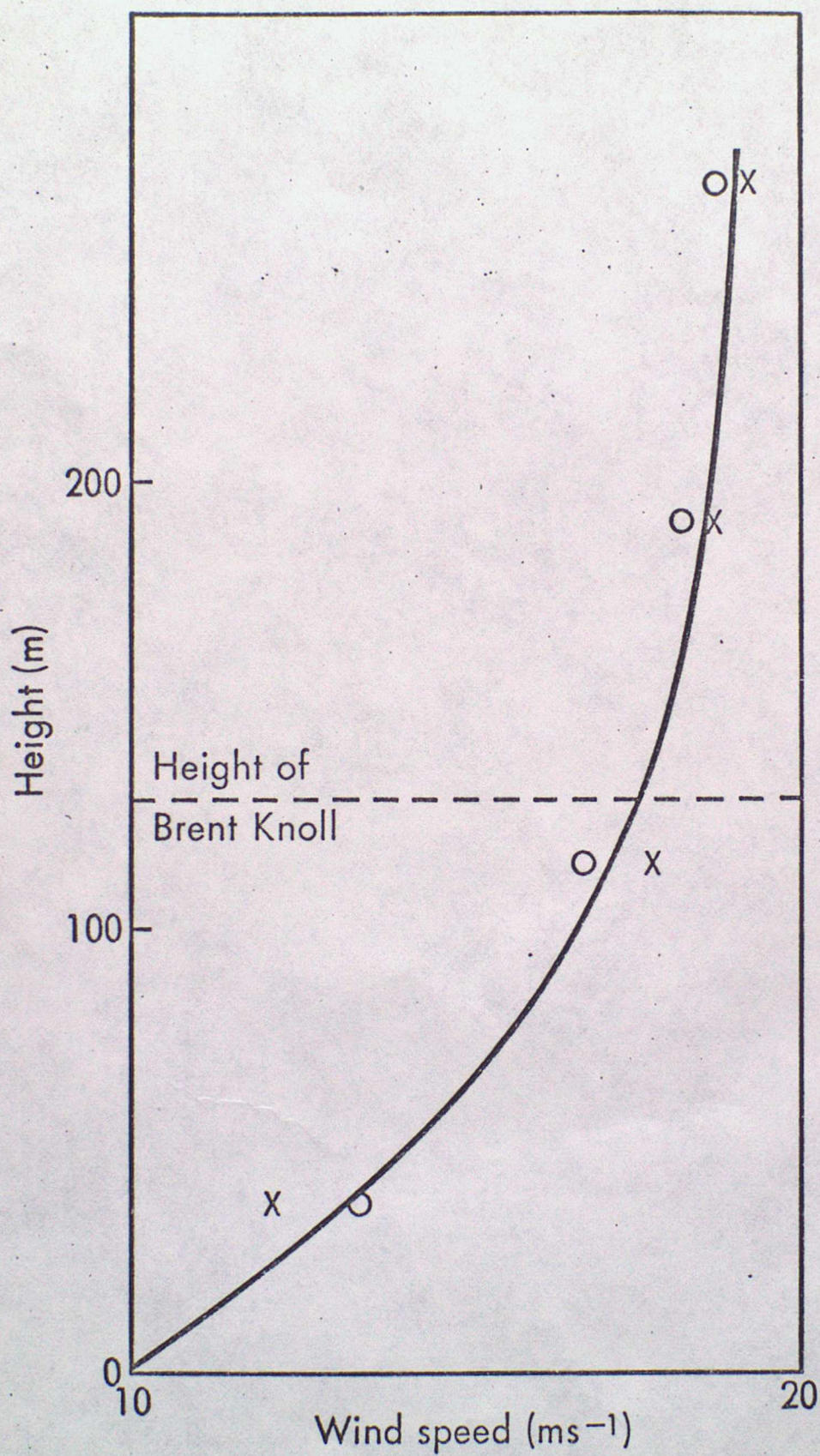


Fig 8

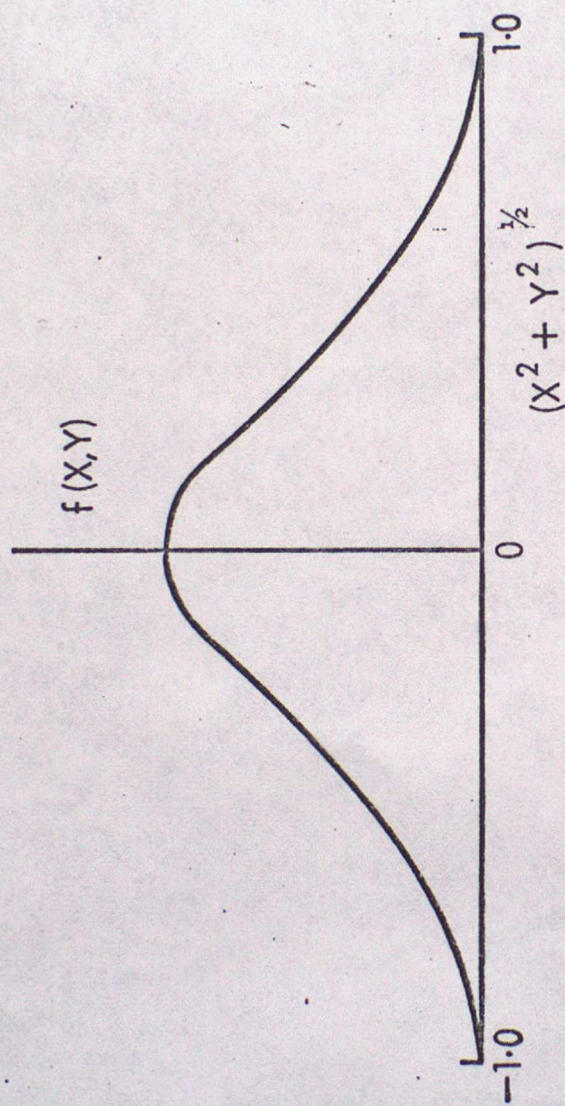
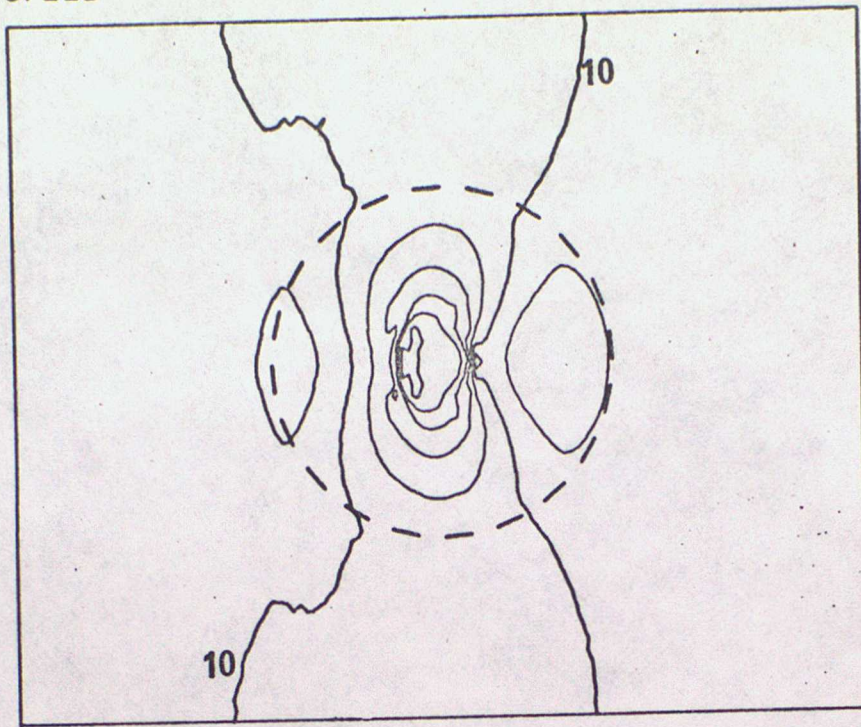


Fig 9

SPEED



DIRECTIONS

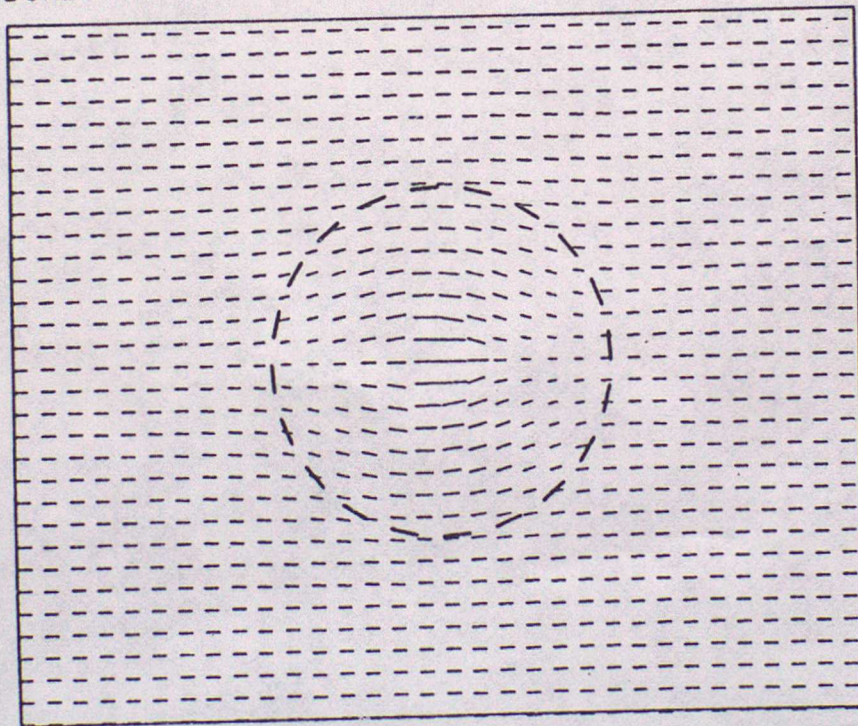


Fig 10